INTERNATIONAL JOURNAL OF CLIMATOLOGY
Int. J. Climatol. **33**: 2758–2767 (2013)
Published online 1 November 2012 in Wiley Online Library
(wileyonlinelibrary.com) DOI: 10.1002/joc.3618

RMetS
Royal Meteorological Society

Short Communication

Cold surge episodes over southeastern Brazil – a potential vorticity perspective

Michael Sprenger,[a]* Olivia Martius[a,b] and Julian Arnold[a]

[a] *Institute for Atmospheric and Climate Science, ETH Zurich, Zurich, CH-8092, Switzerland*
[b] *Oeschger Centre for Climate Change Research and Institute of Geography, University of Bern, Bern, Switzerland*

ABSTRACT: Most intense cold surges and associated frost events in southern and southeastern Brazil are characterized by a large amplitude trough over South America extending toward tropical latitudes and a ridge to the west of it over the Pacific Ocean. In this study, potential vorticity (PV) streamers serve to examine the flow condition leading to cold surges. Case studies suggest that several PV anomalies are related to cold surge episodes: (1) the potential vorticity unit (2-PVU) isoline upstream of South America becomes progressively more distorted prior and during the cold surge episode, indicating a flow situation which is conducive for Rossby wave breaking and hence a flow which strongly deviates from zonality; (2) the initial stage of a cold surge episode is characterized by a northward bulging of high-PV air to the east of the Andes, resulting in a PV streamer whose northern end reaches Uruguay and southeastern Brazil; the strong PV gradient on its western flank constitutes a flow configuration that induces and maintains the transport of sub-Antarctic air toward the subtropics; (3) a distinct negative PV anomaly, a blocking, originates over the eastern South Pacific, upstream of the South America sector. A composite analysis of 27 cold surges is performed for stratospheric PV streamer frequency on several isentropic surfaces. It reveals that equatorward wave breaking over South America and the western South Atlantic represents an important potential component of the dynamics of intense cold surges. The indications are most pronounced around the isentropic levels of 320 K and immediately before the day with largest temperature drops over subtropical Brazil.

KEY WORDS cold surge; potential vorticity; Rossby wave breaking

Received 31 January 2012; Revised 30 July 2012; Accepted 26 September 2012

1. Introduction

Climatologically the equatorward transport of cold air masses in the Southern Hemisphere is largest in the eastern part of South America (Seluchi and Marengo, 2000). Rapid equatorward advection of cold air from sub-Antarctic to subtropical regions is favoured by the synoptic weather situation, the equatorward extension of the sea ice cover in the austral winter and the channelling effect of the Andes (Garreaud an Wallace, 1998; Garreaud 1999, 2000). These transient incursions of Antarctic air into the subtropics to the east of the Andes occur year round with a weekly or biweekly frequency (Marengo and Rogers, 2001). They are a distinctive/ubiquitous feature of the synoptic climatology over this region and are called cold surges. Summertime episodes produce less marked fluctuations of temperature, but they organize convective activity and rainfall in the form of synoptic-scale bands of enhanced deep convection along the leading edge of the cool air (Garreaud, 2000). During wintertime they have a profound impact upon the low-level temperature field and can trigger equatorial Kelvin waves (Liebmann et al., 2009). Occasionally, cold polar air is transported as far as southeastern Brazil and the Amazon region. These events can produce freezing conditions in the coffee growing areas of southern, southeastern and central Brazil and lead to substantial cooling in the Amazon basin (Marengo et al., 1997b). A cold surge extending into the Amazon basin is known locally as 'friagem' (friagen in plural). In 111 years, from 1890 to 2001, 20 friagen were registered. Of these, six were considered catastrophic, the 1902, 1918, 1975, 1981, 1994 and 2000 events (Marengo et al., 2002).

Most cold surges and associated frost events in southern and southeastern Brazil are characterized by distinct features of the large-scale flow over an extensive part of the Southern Hemisphere (Müller and Ambrizzi, 2007). At middle- and upper-levels, a large amplitude mid-latitude trough extends towards the tropical regions of South America and a ridge is located to the west over the Pacific Ocean. A second prominent trough is generally observed upstream in the central Pacific to the east

* Correspondence to: M. Sprenger, Institute for Climate and Atmospheric Science, ETH Zurich, Zurich, Switzerland. E-mail: michael.sprenger@env.ethz.ch

of 180°W (Müller et al., 2005). This Rossby wave-like pattern undergoes a significant meridional amplification before and during the mature stage of the cold surge, and the ridge and trough axes assume a NW–SE orientation when moving to the lee of the Andes (Garreaud, 2000). Krishnamurti et al. (1999) showed that downstream propagation of waves across the Pacific during days prior to the freeze event generally precedes the stronger frost events in southeastern Brazil. The precursor wave signal consisted of superimposed fast-moving synoptic-scale waves and planetary-scale waves. The latter become quasi-stationary during the freeze/cold surge events. The study further showed that these waves interact via energy exchange from the quasi-stationary long waves toward the shorter waves. Krishnamurti et al. (1999) inferred that this conduces to the build-up of the large amplitude trough over South America.

Downstream amplification (expressed as intensifying troughs and ridges) across the Pacific into South America preceded the majority of the heavy frost events over subtropical Brazil (Marengo et al., 2002). Through observational analysis and numerical simulations, Marengo et al. (2002) identified possible forcing mechanisms of the wave trains propagating across the Pacific into South America. Their study suggests that convective forcing with the right amplitude and at the right position may generate a quasi-stationary Rossby wave pattern, which is dynamically relevant for the strong surface cooling over southeastern Brazil. Besides convective forcing, there are other mechanisms how Rossby waves can be initiated or intensified on a tropopause level wave guide (here the southern hemisphere subtropical jet, tropopause on an isentropic surface). One example is stratospheric high-PV (potential vorticity) anomalies that can reach the wave guide from the polar regions. As an example, Dirren and Davies (2004) showed how a stratospheric high-PV anomaly strongly distorted the isentropic tropopause and thus induced low-level cyclogenesis. In a subsequent analysis, Kew et al. (2010) investigated the frequency and dynamics of lower-stratospheric, localized PV anomalies in the Northern Hemisphere. All in all, these studies indicate that the PV perspective might give new insight into the dynamics of friagem. Indeed, it offers several advantages over the more traditional analysis based on geopotential and temperature: (1) gradients of PV act as waveguides for planetary and synoptic-scale Rossby waves (e.g. Schwierz et al., 2004a), (2) upper-level PV anomalies can serve as Rossby wave triggers and (3) upper-level PV anomalies directly affect the surface flow and temperature fields (Hoskins et al., 1985) – a positive stratospheric PV anomaly at upper-levels going along with a negative temperature anomaly underneath (e.g. Schlemmer et al., 2010),

Motivated by these advantages, the aim of this study is twofold: (a) In a first step, we direct the view from more traditional weather charts, as e.g. geopotential height and temperature maps, to the PV perspective (Hoskins et al., 1985). It will be shown in several case studies that the cold surge episodes are associated with a progressively more distorted dynamical tropopause, which finally exhibits characteristic filamentary equatorward excursions of stratospheric high-PV air. These so-called stratospheric PV streamers (Appenzeller and Davies, 1992; Wernli and Sprenger, 2007; Martius et al., 2008) mark the final stage in the life cycle of a Rossby wave; (b) the second step will establish the link between the cold surge episodes and PV streamers in a climatological sense. To this end a 40-year climatology of PV streamers is analyzed for 27 cold surge events between 1983 and 1996.

The PV perspective gained a lot of interest since the landmark paper by Hoskins et al. (1985). The particular link to mountain meteorology, which encompasses South American cold surges, was made in several studies, which now will be shortly outlined. For instance, Martius et al. (2006b) and Hoinka and Davies (2007) investigate how heavy precipitation events on the Alpine south side relate to upper-level PV streamers. A link to other geographical regions, e.g. Israel and Algeria, was also found, see references in Hoinka and Davies (2007). Lee cyclogenesis is another process related to upper-level PV anomalies: Aebischer and Schär (1998) and Tsidulko and Alpert (2001) suggest that the wrapping up of upper-level PV streamers and subsequent interaction with low-level PV structures significantly contributes to Alpine Lee cyclogenesis. Whereas, the previous studies focused on the impact of upper-level PV structures on the low-level flow, the feedback from mountains flows on the large-scale flow can also be adequately described in the PV perspective. In a nutshell, the orographic flow disturbs the PV waveguide (e.g. Schwierz et al., 2004a and references therein) or disrupts an upper-level PV streamer (Morgenstern and Davies, 1999), a distortion which then might translate far downstream. Finally, PV is often found in textbooks about dynamic meteorology, e.g. in Holton (2004), to discuss the differences in westerly and easterly flow impinging on mountains, where only the westerly flow induces wave-like oscillations downstream of the obstacle.

While every cold surge event is triggered by a complex interplay between large-scale flow patterns and anomalies and local forcing, we specifically focus on the large-scale (synoptic) forcing. The meso-scale perspective is discussed for example in Marengo et al. (2002). Furthermore, in addition to the mechanisms leading to friagen presented in this study, i.e. the amplification of wave trains upstream of South America, several other mechanisms have been shown to be important: Reason (1994) investigate the equatorward propagation of orographically trapped disturbances (Kelvin waves), which are excited during the passage of synoptic-scale wave trains over South America; Mailler and Lott (2010) consider the mountain forcing and build-up of a cold dome which then is advected equatorward; Mysak (1980) and Pedlosky (1987) look at topographic Rossby waves, which are the atmospheric pendant to oceanic shelf waves and might propagate along the Andes; Colle and Mass (1995) and Garreaud (2000) focus on nonlinear advection; and finally, Takaya and Nakamura (2005)

looked at cold air advection driven by upper-level PV anomalies, which – using a PV inversion – they found to be important for Asian cold surges. A good overview of different cold surge mechanisms, although for the Asia, is given in Compo et al. (1999).

The study is organized as follows: In Section 2 the data and methodology is presented. Section 3 presents detailed case studies of cold surge events, with focus on the PV perspective. Then, the link between cold surges and PV streamers is established in a climatological sense (Section 4). Finally, some conclusions are drawn in Section 5.

2. Data and methodology

This study focuses on the satellite period (1980–2000) of the ERA-40 reanalysis data set of the European Centre for Medium-Range Weather Forecasts (ECMWF) (Uppala et al., 2005), for which the southern hemispheric flow is well represented in the re-analysis. The primary meteorological fields (horizontal and vertical wind components, temperature, specific humidity and pressure) were interpolated onto a geographical grid with $1^\circ \times 1^\circ$ horizontal resolution. Secondary fields, in particular PV and potential temperature, were calculated on the model grid and then interpolated on pressure and isentropic surfaces. Note that PV is negative in the Southern Hemisphere, however we will refer to stratospheric air ($\mathrm{PV} < -2$ PVU) as high-PV air and to tropospheric air as low-PV air (in an absolute sense).

Breaking Rossby waves (i.e. stratospheric PV streamers) were identified in the ERA-40 data set using an objective algorithm, which detects narrow filaments of high-PV air extending equatorward and low-PV filaments extending poleward. These structures typically form during the final phase of a baroclinic life cycle, when nonlinear effects lead to irreversible distortions of the dynamical tropopause (here defined as the 2-PVU isosurface). The PV streamers were detected every 6 h on a stack of isentropic surfaces (from 300 to 350 K, in steps of 10 K) by an algorithm developed by Wernli and Sprenger (2007) with some minor improvements added (for details, see Appendix A). The output of this algorithm are binary fields indicating the presence or absence of PV streamers at every grid point. The binary fields were then converted into a PV streamer frequency climatology.

Finally, cold surge days are compiled based on data and information given in Marengo et al. (1997a,1997b) and Krishnamurti et al. (1999). In total, 27 cases between 1983 and 1996 are identified and the 'verifying' day is taken to be the one with the largest temperature drop over southeastern Brazil. Apart from four dates in the late autumn, all belong to the southern winter season. A complete list of all cold surges is given in Table 1.

Table 1. Cold surge events used in the composite analysis. This compilation is based on data and information given in Marengo et al. (1997a,1997b) and Krishnamurti et al. (1999). In the composite analysis in Figures 4 and 5, these dates correspond to day 0.

07/06/1983	15/06/1983	03/08/1983
24/08/1984	06/06/1985	02/06/1986
26/07/1986	19/06/1987	26/05/1988
06/06/1988	13/07/1988	26/07/1988
27/05/1989	07/07/1989	19/05/1990
22/05/1990	22/07/1990	28/07/1990
24/07/1992	15/06/1993	08/07/1993
01/08/1993	26/06/1994	09/07/1994
10/08/1994	19/04/1996	05/08/1996

3. Case study

3.1. Synoptic weather charts

Figure 1 illustrates the striking northward progression of a cold front that occurred in June 1994 over South America (June 26 event in Table 1). Shown are equivalent potential temperature θ_e and geopotential height at 850 hPa from 1200 UTC, 24 June to 1200 UTC, 27 June. An anticyclone (label A) was located to the west of Chile on 24 June and a trough was located near the coast of Argentina and Uruguay along 45°W (label B). The trough was associated with an intense cold front that extended into southern-most Brazil. At 1200 UTC, 25 June (Figure 1b), the anticyclone approached the Andes and reached its northern-most position. Cold air entered the continent from the southwest, driven by the cyclonic circulation around low-pressure system B. From 1200 to 1800 UTC, 25 June the cold front over Rio de Janeiro was associated with some cloudiness over southern Amazonia (not shown). On the coldest day, 26 June (Figure 1c), the anticyclone split into two parts (A1 and A2), while the cold front and related cloud band migrated to the northeast. Clear skies behind the cold front led to a dramatic decrease in surface temperatures in southeastern Brazil. Finally, on 27 June (Figure 1d) the cloud band of the front extended from the South Atlantic over eastern to interior Brazil and subsequently dissipated over the continent. The anticyclone A was no longer discernible, and the cyclone B had moved further to the east.

In summary, the cold surge episode was characterized by a distinct synoptic-scale pattern: a strong anticyclone was present to the west of Chile and a cyclone over the South Atlantic. Both contributed to the northward advancement of cold air masses from sub-Antarctic latitudes toward Brazil.

3.2. Isentropic potential vorticity maps

A PV-based analysis of the same June 1994 case is presented in Figure 2. Shown is the time evolution of PV on the 320-K isentrope from 1200 UTC, 23 June to 1200 UTC, 27 June. In order to assess the downstream development, the whole Southern Hemisphere is shown. On 23 June 12 UTC (Figure 2a) two extrusions of high-PV air (i.e. stratospheric PV streamers) were located over the South Pacific Ocean (labels A and B). Over South America, the dynamical tropopause was only weakly disturbed, consistent with a rather zonal flow. Within the following 24 h (Figure 2b,c), the wave

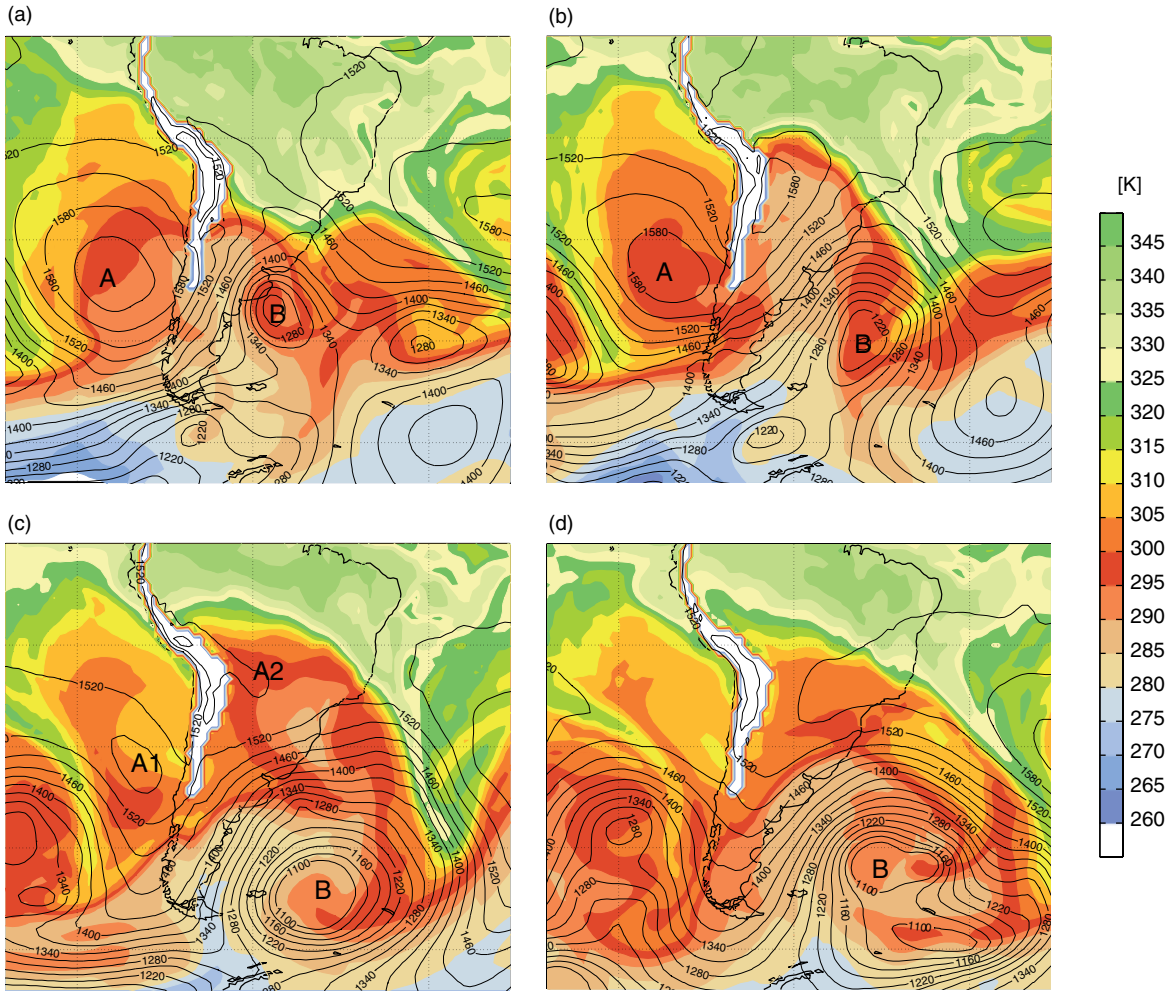

Figure 1. Equivalent potential temperature (θ_e, in [K]) and geopotential height (Z, in [gpm]) at 850 hPa: (a) 1200 UTC, 24 June 1994; (b) 1200 UTC, 25 June 1994; (c) 1200 UTC, 26 June 1994; and (d) 1200 UTC, 27 June 1994.

pattern considerably intensified over the South Pacific and also over South America, now forming a succession of three narrow PV streamers between New Zealand and South America (labels A–C). In between, two intense PV ridges (negative PV anomalies) are discernible, one immediately upstream of South America (F) and one in the central South Pacific (G), see Figure 2d.

The strong PV ridge (F) in conjunction with the pronounced downstream stratospheric PV streamer (C), located over Argentina and extending to 25°S, strengthened the equatorward advection of the cold air (Figure 2e). The formation of the stratospheric PV streamer (C) happened concomitantly with the formation of a surface cyclone over the South Atlantic. The strong PV gradient on the western/upstream edge of the upper-level PV streamer remained quasi-stationary and was oriented almost parallel to the Andes for approximately 36 h (Figure 2d–f). The area of strong cold air advection was colocated with the western edge of the upper-level PV streamer (C). The slow eastward progression of the PV streamer (C) and ridge (F) and its induced equatorward cold air advection are important ingredients of the cold surge event.

Finally, toward the end of the friagem the low-PV ridge to the west of Chile decayed: indicated by the recombination of the isolated PV cutoff (B) with the stratospheric reservoir (Figure 2g–i).

3.3. Downstream development

Krishnamurti et al. (1999) showed that downstream development is aiding the establishment of the synoptic flow configuration over South America that triggers cold surges. The downstream propagation and amplification of a Rossby wave train that preceded the cold surge event of 26 June 1994 is shown in Figure 3, which is a refined Hovmöller diagram of meridional wind on 320 K (Martius et al., 2006a). A precursor Rossby wave signal can be traced back in time and space for approximately 10 d all the way to the southern Atlantic. A first wave ridge formed downstream of South America around June 15. Subsequently a downstream propagating wave train formed (label A). On 21 June over Australia this wave train was caught by and merged with a second, faster moving wave train (label B) and the merged wave subsequently continued its downstream propagation to South America. The wave train interacted

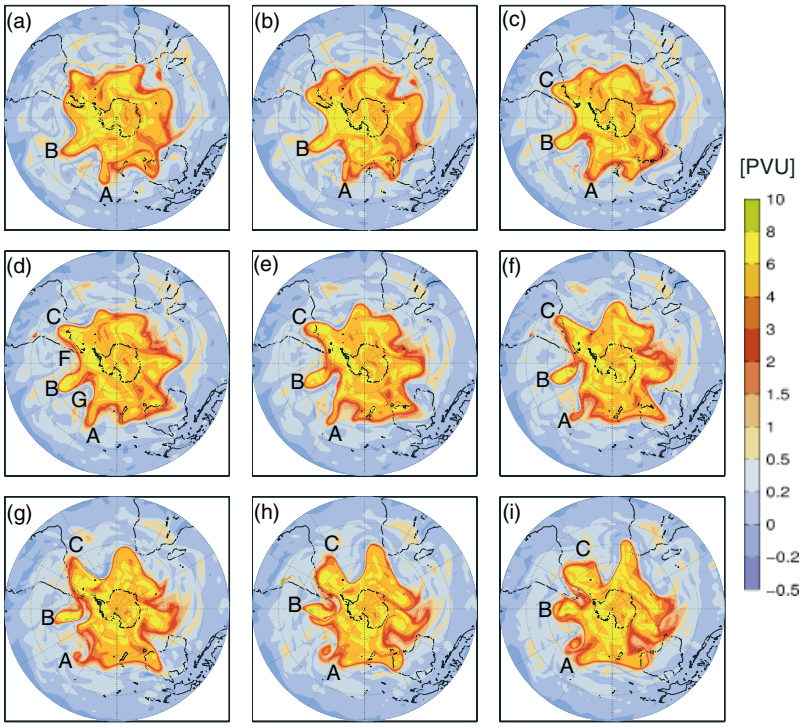

Figure 2. Time sequence of the PV distribution on 320 K (in PVU, bold black line for 2 PVU) for the cold surge event on 26 June 1994, starting from 1200 UTC, 23 June (a) and ending at 1200 UTC, 27 June (i).

with a semi-stationary anticyclone (label C) located in the western Pacific upstream of South America and the waves amplified over South America resulting in the formation of the PV streamer that triggered the cold surge. The relatively stationary high-pressure anticyclone upstream of South America (label C) was also noted by Krishnamurti et al. (1999). In the month of June 1994, the wave train preceding the cold surge event was the only wave train that circled almost the entire Southern Hemisphere. Relative little wave activity was found over the western Pacific during the first 2 weeks of June.

3.4. Synthesis – PV perspective

In the 1994 case study, it was shown that distinct PV features can be associated with friagen in Brazil. In the following, we summarize how the PV perspective (Hoskins et al., 1985) can elucidate the dynamics of these events. Furthermore, possible mechanisms linked to PV thinking are mentioned, although they are not further investigated in this study.

- The dynamical tropopause, i.e. the 2-PVU isoline on an isentropic surface, upstream of and over South America becomes highly distorted prior to and during a cold surge; these distortions become manifest as stratospheric PV streamers. The advantage of the PV perspective lies in the possibility to assess the 'initial' seeds for these PV streamers far upstream. Indeed, it is possible to look for processes which act near the 2-PVU isoline and are able to distort it. Three important processes are: (1) convective updraft which go along with upper-level divergence, leading to an adiabatic displacement of the 2-PVU isoline; (2) diabatic changes of PV due to latent heat release and radiative heating and (3) advection of high-PV air masses from within the stratospheric high-PV reservoir toward the 2-PVU isoline which is distorted by the wind field associated with the high-PV structure. Note that the dynamical tropopause coincides essentially with the jet streams (e.g. Schwierz et al., 2004a) and acts as a waveguide for Rossby waves (Schwierz et al., 2004a).
- A pronounced atmospheric block, which is discernible as a distinct negative PV anomaly at upper-tropospheric levels (Schwierz et al., 2004b), resided to the west of South America during the cold air outbreak. At lower levels, the negative PV anomaly was associated with an anticyclonic flow field which extended far to the south. The anticyclonic circulation contributed to the equatorward advection of cold sub-Antarctic air. Furthermore, the blocking effect of the negative anomaly, i.e. its persistence over several days, helped to maintain a steady southerly flow over South America. The formation of the negative PV anomaly is related to the distorted waveguide mentioned before. It might be stabilized and further intensified by PV destruction associated with warm conveyor belts (e.g. Wernli and Davies, 1997).
- Over the southwest Atlantic and/or South America, a stratospheric PV streamer was present during the cold air outbreak. This PV streamer was located on the eastern edge of the atmospheric block. The associated cyclonic flow at lower-tropospheric levels

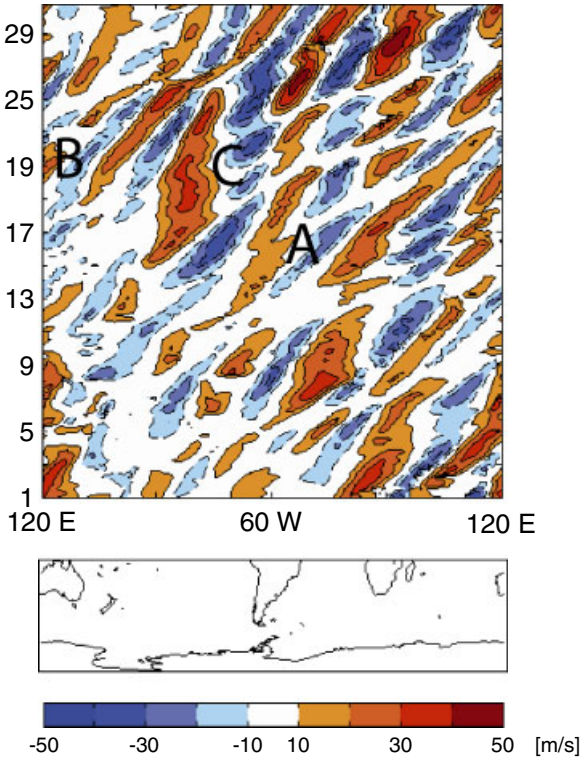

Figure 3. Hovmöller diagram of the meridional wind on 320 K in June 1994.

enhanced the equatorward advection of sub-Antarctic air. Moreover, it remained essentially stationary for 36 h, most likely due to the sheltering effect of the atmospheric blocking to the west of South America. Its western edge was aligned remarkably parallel to the Andes.

4. Climatological aspects

Three additional examples of cold surge episodes affecting southeastern Brazil are briefly discussed (8 June 1985, 7 July 1989, 22 May 1990) to further illustrate the upper-level flow structure and PV streamers that occur in the vicinity of South America prior to and during these events. Shown are the spatial and temporal evolution of stratospheric PV streamers on the 320-K level (Figure 4). The evolution of the stratospheric PV streamers is tracked over a period of 96 h starting 3 d before each event.

On 8 June 1985, an elongated, NW–SE oriented stratospheric PV streamer was present over the western South Atlantic (Figure 4a). Its occurrence coincided with the day of extreme cooling over southeastern Brazil. During the 36-h interval, the PV streamer remained almost stationary, but became laterally compressed. In the friagem from 7 July 1989 (Figure 4b) the stratospheric PV streamer was located to the west of Argentina. In the course of its lifetime of 3 d, the tip moved from the Argentine Pampas to southeastern Brazil where it was located on the day of intense cooling. The evolution of this PV streamer was characterized by a stretching and a gradual turning of its axis from almost N–S to NW–SE. Finally in the third example (Figure 4c), on 22 May 1990, a meridionally to NW–SE oriented stratospheric PV streamer was located over the western South Atlantic. This rapidly growing PV streamer was detected 1 d prior to the largest temperature drops in southeastern Brazil and existed for more than 2 d. Initially, the PV streamer was located over Argentina and Uruguay and then drifted westwards.

To complete and generalize the results from the case studies and from Section 3, this section further presents a compositing analysis of stratospheric PV streamers that occur during cold surge episodes in Brazil. The cases listed in Table 1 have been used to construct composites of the spatial frequency of stratospheric PV streamers (see Section 2 and Table 1). Note that each member of the 27 cases can contribute $1/27 \times 100\%$ to the streamer frequencies in the composite analysis; hence, every approximately 2.5% step in the frequency marks the occurrence of an additional PV streamer identified.

The climatological frequency of occurrence of stratospheric PV streamers during JJA around South America is discussed first (contour lines in Figure 5). The climatological maximum with values above 8% frequency is broadest over South America and extends eastwards for 2000 km, becoming progressively narrower leewards of the Andes. Such a configuration indicates a possible orographic influence on PV streamer formation and occurrence.

The frequency of stratospheric PV streamers on 320 K at the day of the cold surge (according to Table 1) is indicated by the grey shading in Figure 5c. Compared to the climatology, the frequency maximum in the cold surge composites possesses a statistically significant different location and amplitude. It takes the form of a NW–SE aligned, tongue-shaped structure pointing toward subtropical Brazil. The form, position and orientation of this structure resemble the stratospheric PV streamers shown previously for three cases (Figure 4). The amplitude reaches values of up to 30% in the composite, i.e. in 30% of the cold surge events the region is occupied by a stratospheric PV streamer. These values exceed the corresponding climatological frequency about three times. The percentage of 30% is also confirmed if the PV fields for all 28 members of the composite are considered: according to a subjective inspection, 11 cases are clearly associated with PV streamers on the day of the cold surge and for about 8 further cases, streamer-like distortions of the tropopause are discernible.

The temporal evolution of the stratospheric PV streamers is interesting as well (Figure 5a–d). Two days before the cold surge, a maximum in the streamer frequency is already discernible in the composite (Figure 5b). The maximum is slightly shifted to the west compared to day 0, indicating a slow eastward shift, and the amplitude is already very high (up to 30%). Hence, stratospheric PV streamers associated with cold surges and intense cooling over southeastern Brazil tend to occur prior to the day

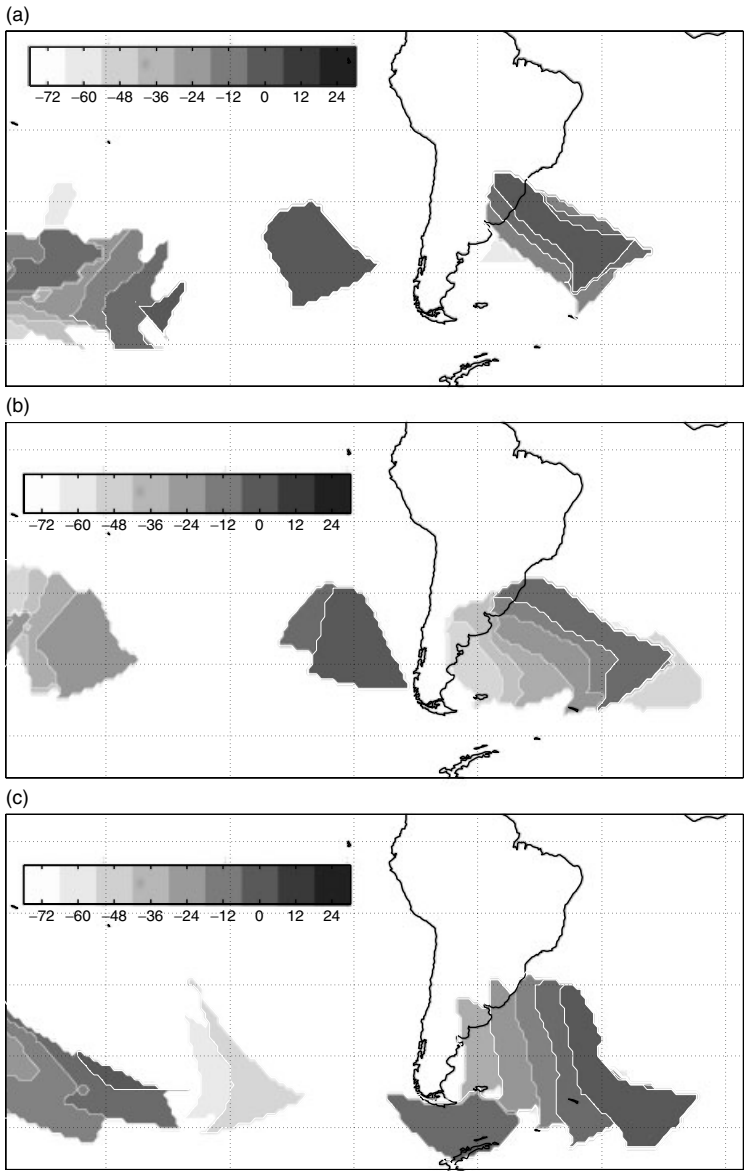

Figure 4. Spatial and temporal evolution of stratospheric PV streamers on 320 K for the cold surge events on (a) 8 June 1985, (b) 7 July 1989 and (c) 22 May 1990. The grey shadings correspond to different times (in hours) relative to the cold surge day: starting 3 d (72 h) before the coldest day and ending at 24 h after it.

with largest temperature drops and remain almost stationary for at least 2 d. Consistent with the observations in the case studies, all the composites show additional areas of enhanced PV streamer occurrence before and after the cold surge episodes. In the composite for day −4 (Figure 5a), several irregularly shaped areas with secondary frequency maxima are present over the South Pacific and Atlantic Ocean. The same is true for the composite for day +2 (Figure 5d), where the PV streamer frequency maximum over South America is shifted to the east, but a new local maximum becomes discernible to the west of South America. In summary, these signals indicate an anomalous Rossby wave breaking activity prior, during and after the cold surge episodes.

To make the link between the PV streamers and the cold air advection more explicit, Figure 6a shows a composite of all events 1 d before the cold surge of low-level wind vectors and equivalent-potential temperature (at 850 hPa), of mid-tropospheric meridional flow (at 500 hPa) and of the dynamical tropopause at 320 K. The PV anomaly in Figure 5b,c now manifests itself as an equatorward distorted tropopause, which by means of the PV inversion principle is associated with a mid-tropospheric equatorward flow on its western flank. Further down, at 850 hPa, this equatorward flow is still discernible and it exhibits a pronounced cross-isothermal component, i.e. it goes along with cold air advection. The influence of the equatorward cold air progression is further supported by 4-d backward trajectories started at 58°W/27°S and at 850 hPa (Figure 6b). Indeed, 70% of the trajectories are coming from region further south than 40°S. For 50°S and 60°S the corresponding percentages become 47% and 20%, respectively.

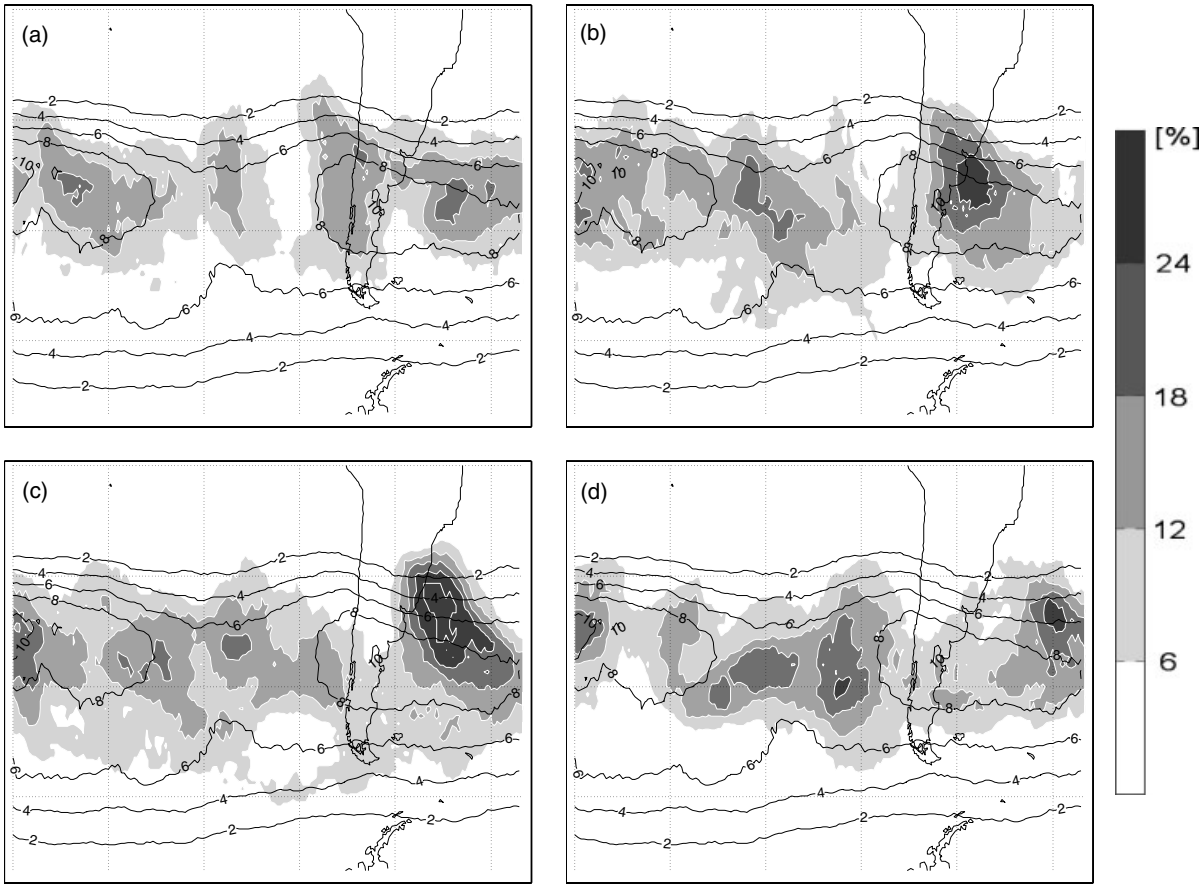

Figure 5. Cold surge composites of the frequency distribution of stratospheric streamers on 320 K (in grey shading): (a) 4 d before, (b) 2 d before, (c) at time of and (d) 2 d after the cold surge (as given in Table 1). For comparison, all panels include the austral winter (JJA) climatology of stratospheric streamers on 320 K (as thin black line).

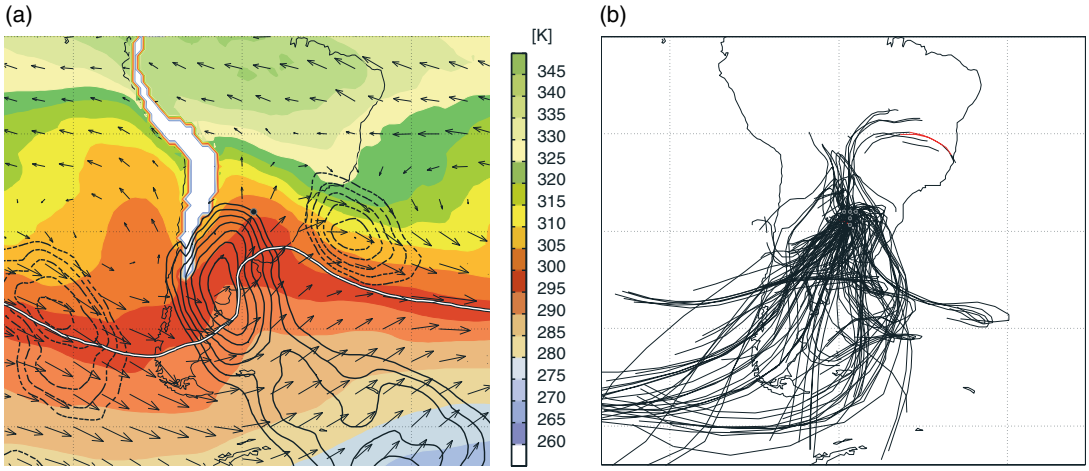

Figure 6. (a) Composite 1 d before the cold surge (see Table 1) of equivalent-potential temperature (in [K]) at 850 hPa, wind vectors at 850 hPa (arrows), meridional wind at 500 hPa (in [m s^{-1}] from 5 m s^{-1} in steps of 1 m s^{-1}, solid equatorward and dashed poleward), and of the 2-PVU isoline at the 320-K isentrope. (b) Four-day backward trajectories started at 58°W/27°S, with four additional start positions displaced 1° east/west and south/north, and at 850 hPa. The trajectories are started at the day of the cold surge (as given in Table 1).

Finally, we shortly discuss the occurrence of PV streamers at levels other than 320 K (not shown). Below the 320-K level the PV streamers are located very far south and are therefore of no dynamical importance for the cold surges. On the isentropic levels of 330 and 340 K, the stratospheric PV streamer frequency becomes considerably reduced but the geographical distributions are consistent with those on the 320-K level. The combined consideration of all isentropic levels, including 320 K, yields two fundamental results. First, with increasing isentropic

height, the streamer frequency is located more equatorward. This is due to the progressive northward shift of the intersection between the isentropic levels of increasing height and the mean dynamical tropopause (Wernli and Sprenger, 2007). Second, the level of 320 K contains the most significant evidence of a linkage between cold surge episodes and PV streamers. This isentropic surface intersects the dynamical tropopause in the subtropics.

5. Discussion and conclusions

This article describes cold air outbreaks over South America from a PV perspective. To this end two different PV-based analyses are presented: (1) a case study of the cold surge event from 26 June 1994 linking the surface weather evolution and upper-level PV structures; (2) a composite analysis of stratospheric PV streamers on the 320-K isentropic surface for 27 cold air events between 1983 and 1994. In the following, the key results are summarized.

a. The case studies reveal that the flow structure of the dynamical tropopause is highly deviates from zonality prior to and during cold surge episodes. Typically several stratospheric PV streamers occur over the South Pacific and over South America, indicating the downstream amplification and breaking of Rossby waves. Furthermore, upstream of South America a pronounced negative PV anomaly is discernible, which goes along with a blocking anticyclone in the more traditional perspective.
b. The composites for stratospheric PV streamer occurrence reveal conspicuous frequency maxima over the western South Atlantic and the South American continent. The NW–SE alignment and the tongue-like shape reflect to some degree the canonical form of stratospheric PV streamer as identified in the case studies over the same region. The structure is particularly pronounced in the composite for the day of the extreme cooling, with a frequency maximum of 36% in its centre to the southeast of subtropical Brazil. Consequently, a stratospheric PV streamer was present there on more than a third of the considered time instants, which by far exceeds the climatological frequency of 8%.
c. While the PV trough over South America progressively lengthens, it migrates to the northeast and transforms into a PV streamer, whose northern end reaches Uruguay and southeastern Brazil. The strong PV gradient on its western flank constitutes a flow configuration that induces and maintains the transport of sub-Antarctic air toward the subtropics. The equatorward transport of sub-Antarctic air is further enhanced by the occurrence of the pronounced low-PV ridge to the west of South America, i.e. the blocking anticyclone. The downstream flow of this low-PV ridge favourably feeds into the 'north–south aligned duct' established by the more easterly stratospheric PV streamer and hence allows a significant northward flow of Antarctic or sub-Antarctic air towards central South America.

To sum up, the results of this study confirm the complexity of the upper-level flow configuration of cold surge episodes. There is a considerable variability regarding the presence and evolution of PV streamers during the course of this atmospheric phenomenon. Despite of this fact, PV streamers over South America and the adjacent ocean are an important component of the dynamics of intense cold surge episodes affecting southeastern Brazil. In a further study it would be fruitful to investigate in greater detail the physical mechanisms which lead to the PV streamer or which enhance pre-existing distortions of the 2-PVU isoline.

6. Appendix A: Streamer Identification Algorithm

The identification of the stratospheric streamers is based on the method developed by Wernli and Sprenger (2007). The 2-PVU isoline on an isentropic surface, i.e. the dynamical tropopause on that surface, is determined. The algorithm yields the line as a set of latitude/longitude coordinates which are approximately 50 km separated from each other. The identification of the streamers along this contours is split into three distinct steps.

1. Two points along the contour are searched which are separated by at most 1500 km along a semi-circle on the globe and by at least 2000 km along the 2-PVU line. This first criterion captures an essential characteristic of a stratospheric streamer, i.e. first its narrow structure and hence close neighbourhood of two points and second its filamentary structure and hence the elongated 2-PVU contour length between two points. At the end of this step, a section of the 2-PVU contour between two close-encountering points is marked as a potential PV streamer.
2. The marked section is extended polewards at its left and right edge. Indeed, the two close-encountering points, which are at most 1500 km apart, might well be in the 'middle' of a subjectively identified streamer, particularly if the streamer has a tendency of cutting off its narrow tip. The aim of the second step is the better agreement between the algorithmically and subjectively identified streamers.
3. Some checks are performed in order to eliminate structures, which would not be considered as a streamer if subjective identification is applied. The additional checks are: (1) if the distance between the edge points along the contour is larger than 15 000 km, the structure is no longer considered as a streamer candidate, although a substructure along this contour section might still be accepted as a streamer, (2) the distance along the contour must be at least twice as large as the semi-circle distance between the end points and (3) if more than 80% of the 2-PVU contour is identified as streamer, no streamer at

all is accepted along this contour. Note that the last criterion applies to very distorted 2-PVU contours, as they might occur at low-lying isentropes with a 'flat' intersection with the 2-PVU isosurface.

All in all, this results in a robust methodology results for objective streamer identification. Visual inspection of many cases proofed the algorithm's power in finding stratospheric streamers and in yielding a good agreement to subjectively identified streamers. It is particularly the second aspect where differences to the method by Wernli and Sprenger (2007) exist. A comparison between the two methods gives very good agreement in geographical patterns, but an increased amplitude for the improved method of this study.

References

Aebischer U, Schär C. 1998. Low-level potential vorticity and cyclogenesis to the Lee of the Alps. *Journal of the Atmospheric Sciences* **55**: 186–207. DOI: 10.1175/1520-0469(1998)055<0186:LLPVAC>2.0.CO;2.

Appenzeller C, Davies HC. 1992. Structure of stratospheric intrusions into the troposphere. *Nature* **358**: 570–572.

Colle B, Mass CF. 1995. The structure and evolution of cold surges east of the Rocky Mountains. *Monthly Weather Review* **123**: 2577–2610.

Compo GP, Kiladis GN, Webster PJ. 1999. The horizontal and vertical structure of east Asian winter monsoon pressure surges. *Quarterly Journal of the Royal Meteorological Society* **125**: 29–54. DOI: 10.1002/qj.49712555304.

Dirren S, Davies HC. 2004. Combined dynamics of boundary and interior perturbations in the Eady setting. *Journal of the Atmospheric Sciences* **61**: 1549–1565.

Garreaud R. 1999. Cold air incursions over subtropical and tropical South America: a numerical case study. *Monthly Weather Review* **127**: 2823–2853.

Garreaud R. 2000. Cold air incursions over subtropical South America: mean structure and dynamics. *Monthly Weather Review* **128**: 2544–2559.

Garreaud R, Wallace J. 1998. Summertime incursions of midlatitude air into subtropical and tropical South America. *Monthly Weather Review* **126**: 2713–2733.

Hoinka KP, Davies HC. 2007. Upper-tropospheric flow features and the Alps: an overview. *Quarterly Journal of the Royal Meteorological Society* **133**: 847–865. DOI: 10.1002/qj.69.

Holton JR. 2004. *An Introduction to Dynamic Meteorology*. Elsevier Academic Press: Amsterdam.

Hoskins B, McIntyre M, Robertson A. 1985. On the use and significance of isentropic potential vorticity maps. *Quarterly Journal of the Royal Meteorological Society* **111**: 877–946.

Kew S, Sprenger M, Davies HC. 2010. Potential vorticity anomalies of the lowermost stratosphere: a 10-yr winter climatology. *Monthly Weather Review* **13**: 1234–1249.

Krishnamurti T, Tewari M, Chakraborty D, Marengo J, Silva Dias P, Satyamurty R. 1999. Downstream amplification: a possible precursor to major freeze events over southeastern Brazil. *Weather and Forecasting* **14**: 242–270.

Liebmann B, Kiladis GN, Carvalho LMV, Jones C, Vera CS, Bladé I, Allured D. 2009. Origin of convectively coupled Kelvin Waves over South America. *Journal of Climate* **22**: 300–315. DOI: 10.1175/2008JCLI2340.1.

Mailler S, Lott F. 2010. Equatorial mountain torques and cold surge preconditioning. *Journal of the Atmospheric Sciences* **67**: 2101–2120.

Marengo J, Rogers J. 2001. Polar air outbreaks in the Americas: assessments and impacts during modern and past climates. In *Interhemispheric Climate Linkages*, Markgraf V (ed). Academic Press: San Diego; 31–51.

Marengo J, Cornejo A, Satyamurty P, Nobre C, Sea W. 1997a. Cold surges in tropical and extratropical South America: the strong event in June 1994. *Monthly Weather Review* **125**: 2759–2786.

Marengo J, Nobre C, Culf A. 1997b. Climatic impacts of "Friagens" in forested and deforested areas of the Amazon Basin. *Journal of Applied Meteorology* **36**: 1553–1566.

Marengo J, Ambrizzi T, Kiladis G, Liebmann B. 2002. Upper-air wave trains over the Pacific Ocean and wintertime cold surges in tropical-subtropical South America leading to freezes in southern and southeastern Brazil. *Theoretical and Applied Climatology* **73**: 223–242.

Martius O, Schwierz C, Davies HC. 2006a. A refined Hovmöller diagram. *Tellus A* **58**: 221–226.

Martius O, Zenklusen E, Schwierz C, Davies HC. 2006b. Episodes of alpine heavy precipitation with an overlying elongated stratospheric intrusion: a climatology. *International Journal of Climatology* **26**: 1149–1164. DOI: 10.1002/joc.1295.

Martius O, Schwierz C, Sprenger M. 2008. Dynamical tropopause variability and potential vorticity streamers in the Northern Hemisphere – a climatological analysis. *Advances in Atmospheric Science* **25**: 367–380. DOI: 10.1007/s00376-008-0367-z.

Morgenstern O, Davies HC. 1999. Disruption of an upper-level PV-streamer by orographic and cloud-diabatic effects. *Contributions to Atmospheric Physics* **72**: 173–186.

Müller G, Ambrizzi T. 2007. Teleconnection patterns and Rossby wave propagation associated to generalized frosts over southern South America. *Climate Dynamics* **29**: 633–645.

Müller G, Ambrizzi T, Nunez M. 2005. Mean atmospheric circulation leading to generalized frosts in central southern South America. *Theoretical and Applied Climatology* **82**: 95–112.

Mysak LA. 1980. Recent advances in shelf wave dynamics. *Reviews of Geophysics and Space Physics* **18**: 211–241.

Pedlosky J. 1987. *Geophysical Fluid Dynamics*. Springer-Verlag: New York.

Reason CJC. 1994. Orographically trapped disturbances in the lower atmosphere: scale analysis and simple models. *Meteorology and Atmospheric Physics* **53**: 131–136.

Schlemmer L, Martius O, Sprenger M, Schwierz C, Twitchett A. 2010. Disentangling the forcing mechanisms of a heavy precipitation event along the Alpine south side using potential vorticity inversion. *Monthly Weather Review* **138**: 2336–2353. DOI: 10.1175/2009MWR3202.1.

Schwierz C, Dirren S, Davies HC. 2004a. Forced waves on a zonally aligned jet stream. *Journal of the Atmospheric Sciences* **61**, 73–87. DOI: 10.1175/1520-0469(2004)061<0073:FWOAZA>2.0.CO;2.

Schwierz C, Croci-Maspoli M, Davies HC. 2004b. Perspicacious indicators of atmospheric blocking. *Geophysical Research Letters* **31**: L06125. DOI: 10.1029/2003GL019341.

Seluchi M, Marengo J. 2000. Tropical-midlatitude exchange of air masses during summer and winter in South America: climatic aspects and examples of intense events. *International Journal of Climatology* **20**: 1167–1190.

Takaya K, Nakamura H. 2005. Mechanisms of intraseasonal amplification of the cold Siberian High. *Journal of the Atmospheric Sciences* **62**: 4423–4440. DOI: 10.1175/JAS3629.1.

Tsidulko M, Alpert P. 2001. Synergism of upper-level potential vorticity and mountains in Genoa lee cyclogenesis – a numerical study. *Meteorology and Atmospheric Physics* **78**: 261–285. DOI: 10.1007/s703-001-8178-8.

Uppala SM, Kallberg PW, Simmons AJ, Andrae U, Da Costa Bechtold V, Fiorino M, Gibson JK, Haseler J, Hernandez A, Kelly GA, Li X, Onogi K, Saarinen S, Sokka N, Allan RP, Andersson E, Arpe K, Balmaseda MA, Beljaars ACM, Van De Berg L, Bidlot J, Bormann N, Caires S, Chevallier F, Dethof A, Dragosavac M, Fisher M, Fuentes M, Hagemann S, Hólm E, Hoskins BJ, Isaksen L, Janssen PAEM, Jenne R, Mcnally AP, Mahfouf J-F, Morcrette J-J, Rayner NA, Saunders RW, Simon P, Sterl A, Trenberth KE, Untch A, Vasiljevic D, Viterbo P, Woollen J. 2005. The ERA-40 re-analysis. *Quarterly Journal of the Royal Meteorological Society* **131**: 2961–3012.

Wernli H, Davies HC. 1997. A Lagrangian-based analysis of extratropical cyclones. I: the method and some applications. *Quarterly Journal of the Royal Meteorological Society* **123**: 467–489.

Wernli H, Sprenger M. 2007. Identification and ERA-15 climatology of potential vorticity streamers and cutoffs near the extratropical tropopause. *Journal of the Atmospheric Sciences* **64**: 1569–1580.

